AIMS Materials Science, 10(4): 556–574.
DOI: 10.3934/matersci.2023031
Received: 13 May 2023
Revised: 15 June 2023
Accepted: 25 June 2023
Published: 21 July 2023

http://www.aimspress.com/journal/Materials

Research article

Ethylene-propylene-diene (EPDM) rubber/borax composite: kinetic thermal studies

Alaa Ebrahiem[1], Sobhy S Ibrahim[1,*], Ahmed M El-Khaib[2] and Ahmed S Doma[3]

[1] Physics Department, Faculty of Science, Cairo University, Giza, Egypt
[2] Physics Department, Faculty of Science, Alexandria University, Alexandria 21511, Egypt
[3] Advanced Technology and New Materials Research Institute (ATNMRI), City of Scientific Research and Technological Applications (SRTA-City), New Borg Al-Arab City, 21934 Alexandria, Egypt

*** Correspondence:** Email: sobhy2000.01@gmail.com.

Abstract: This research studies the effect of borax on the thermal stability and thermal kinetic behavior of ethylene-propylene-diene (EPDM) rubber composites. Using a laboratory two-roll mill at room temperature, carbon-black (N-220) as filler, and other additives such as zinc oxide, stearic acid, and paraffin oil were incorporated into the EPDM rubber matrix. The composite was prepared at different borax concentrations (25 and 50 phr). Thermogravimetric analysis was performed to characterize borax's effect onthermal stability before and after borax addition. Added borax to the host composite rubber (EPDM composite without borax) significantly improved the composite's thermal stability. Borax-loaded composites behave differently at various temperatures. To investigate the kinetic-thermal analysis of the prepared samples, three different models were applied. The activation energy (Ea) and frequency factors (A) for the Horowitz-Metzger, Broido and Coats-Redfern models were calculated. These models were compared and discussed based on their results. First-order decomposition also represented the main decomposition stage. Kraus and Cunnen-Russel models were used to test the interaction between rubber and borax based on previously published swelling results. No interaction was found between rubber and borax.

Keywords: EPDM; rubber composite; thermal stability; kinetic thermal analysis; borax; kinetic models; Horowitz-Metzger; Broido model; Coats-Redfern

1. Introduction

In many heavy industries, different types of rubber are used for different applications (e.g., thermal insulation, leak prevention, etc.). These applications include shielding against ionizing radiation and neutrons. EPDM rubber is one of the most popular rubber types used for these purposes. EPDM rubber is preferable for radiation shielding when adding boron compounds or derivatives. These compounds absorb radiation or convert it to lower-energy radiation. When using these materials for such purposes, it is worthwhile to study their thermal stability. In addition, it is worthwhile to study the effect of different weight ratios of additives on their thermal stability.

Ethylene-propylene diene terpolymer (EPDM) is a type of rubber produced from ethylene, propylene and non-conjugated diene (EPDM). It can act as a suitable heat-insulator binder because it has a glass transition temperature of −50 ℃ and a thermal conductivity of around 0.25 W/(m·K). Long shelf life and exceptional low-temperature performance are two more key features of EPDM. On the other hand, EPDM's char yield and ablation resistance are quite low and require the strengthening of fillers. One of the main fillers used to improve elastomers' electrical and mechanical properties is carbon black.

Farajpour et al. [1] investigated the effect of borax on the mechanical and ablation properties of three different EPDM compounds containing 10 phr of carbon fibre, Kevlar, or carbon fibre/Kevlar. Fumed silica powder (30 phr) and paraffin oil (10 phr) were used in all formulations. Adding borax to composite samples containing carbon fibre or Kevlar fibre or their equal ratio mixture increased tensile strength, elastic modulus and hardness while slightly decreasing elongation at break. The TGA results revealed that borax added to rubber compounds increased char yield at 670 ℃ significantly. The effect of loading high-density polyethylene with boron-based fire retardants and fibre on the mechanical, fire and thermal performances of impregnated spruce wood floors was investigated by Cavdar et al. [2]. According to their findings, samples with borax provided better mechanical properties than samples with boric acid. They showed a 19% improvement in tensile modulus for 40% fibre loadings compared to control samples.

Many studies have been conducted to take advantage of borax to improve thermal conductivity and as a fire retardant agent in materials [3–5]. Also, borax was used as a reinforced compound to enhance polymers and rubbers' thermal and mechanical properties [6–9]. In the fields of nuclear energy, radiation therapy and the aerospace industry, flexible rubber composite materials are applied in the manufacture of walls to prevent the escaping neutrons. They also absorb emitted radiation [10–12]. For this purpose, many researchers were interested in using EPDM rubber loaded with carbon (fibre, powder or nanotubes) and other materials at specific concentrations for radiation shielding and neutron suppression [13]. Those materials include boron and its derivatives [14,15].

There are several studies that have studied the thermal stability of EPDM rubber loaded fillers and a minimal investigation on the kinetic thermal analysis using the thermal gravimetricanalysis [16–18]. For vulcanized EPDM loaded with different phr of borax, few articles were found related to such composite [1,8], and we have to know the effect of borax on the thermal behavior and decomposition mechanisms of the composite compared to raw rubber.

In this research, we focus on the study of gravimetric decomposition analysis (TGA) of EPDM rubber composites with different borax ratios. Three different borax concentrations (0, 25 and 50 phr of borax) were prepared. Possible decomposition mechanisms were also investigated to get better

information about the decomposition of such composites. In addition, they were investigated to show the effect of borax on the composite's thermal behavior.

2. Theoretical approach

2.1. Kinetic thermal analysis

For TGA measurement, the decomposition rate or the conversion (alpha) is given based on Eq 1,

$$\alpha = \frac{m_0 - m_t}{m_0 - m_f} \tag{1}$$

where m_0, m_t and m_f represent the sample's initial weight, residual weight at time t and final weight, respectively. The rate of conversion (dα/dt) is given by Eq 2,

$$\frac{d\alpha}{dt} = kf(\alpha) \tag{2}$$

where k is the rate constant, and f(α) is the conversion function. The conversion function (Eq 3) is directly proportional to the amount of non-decomposed material and can be represented as

$$f(\alpha) = (1 - \alpha)^n \tag{3}$$

where n represents the order of the reaction. The Arrhenius formulation can be used to describe the temperature dependency of the rate constant (Eq 4) and it is given as

$$k = Aexp(\frac{-E}{RT}) \tag{4}$$

where, E is the apparent activation energy, A is the pre-exponential factor, R is the gas constant and T is the absolute temperature. By substituting in the previous equations (Eq 4) and replacing the differentiation from dt (time) to dT (temperature), we get

$$\frac{d\alpha}{(1-\alpha)^n} = \frac{A}{\beta}\exp(-\frac{E}{RT})dT \tag{5}$$

By integrating Eq 5, (from the beginning of the reaction temperature to the peak corresponding to the highest reaction rate and from α = 0 to 1), we get the following equation

$$g(\alpha) = \int_0^\alpha \frac{d\alpha}{(1-\alpha)^n} = \frac{A}{\beta}\int_{T_0}^{T} \exp\left(-\frac{E}{RT}\right) dT \tag{6}$$

For solving the above integration (Eq 6), several strategies have been developed. These methods can be divided into two groups; the 1st group employs data from a single heating rate, and the 2nd based on using multi-heating rates. Differential and integral methods can be applied to both types of procedures. The Kissinger [19] and Friedman [20] techniques are differential approaches, while the Flynn-Wall-Ozawa [21,22], Coats-Redfern [22] and Horowitz-Metzger methods [23] are all integral methods.

This research article will investigate a comparison between one of the differential solution models (Friedman model) and the other based on the integral solution models (Coats-Redfern models).

2.1.1. Broido model

The activation energy (Ea) for pyrolysis was calculated using the Broido mathematical model [24]. Broido calculates the activation energy based on the following expression (Eq 7) and assuming a first-order decomposition process:

$$\mathrm{Ln}[\ln(1/Y)] = -(E/RT) + \ln A \tag{7}$$

Where

$$Y = (w_T - w_f)/(w_i - w_f) \tag{8}$$

where in Eq 8, w_T denotes the sample weight at temperature T, w_f denotes the sample's final weight, w_i denotes its initial weight, and Y is the fraction of initial molecules that have not yet decomposed. The activation energy and the constant A can be determined from the most linear fitting region of ln[ln(1/Y)] vs. 1/T.

2.1.2. Horowitz-Metzger model

Typical approximation methods are illustrated by the Horowitz-Metzger equation (Eq 9),

$$\log\left[\frac{\{1-(1-\alpha)^{1-n}\}}{1-n}\right] = \frac{E\theta}{2.303RT_s^2},\ for\ n \neq 1 \tag{9}$$

For n = 1, the left hand side of Eq 9 would be log[−log(1 − α)]. It is conceivable to write the Horowitz Metzger equation (Eq 9) as follows for a first-order kinetic process

$$\log\left(\log\left(\frac{w_f}{w}\right)\right) = \frac{E\theta}{2.303RT_s^2} - log2.303,\ for\ n = 1 \tag{10}$$

Ts is the temperature at which (1 − α) = 0.368, θ = T − Ts, $w = w_f - w_T$, w_f = mass loss at the completion of the reaction $\left(\frac{w_f}{w_T}\right) = 1 - \alpha$.

Using Eq 10, the plot of $\log[log(1-\alpha)]\ vs\ \theta$ or $\ln[ln(1-\alpha)]\ vs\ \theta$ was drawn and found to be linear from the slope of which E can be calculated. The pre-exponential factor, A, was calculated from Eq 11,

$$\frac{E}{RT_s^2} = A/\left[\beta\ \exp(-\frac{E}{RT_s})\right] \tag{11}$$

β is the heating rate.

2.1.3. Coats-Redfern method

The Coats-Redfern model is used in determining the activation energy (E_a) and frequency factor (A) for 1st order decomposition by using the following expression (Eq 12),

$$\ln g(\alpha) = -\frac{E}{RT} + \ln(\frac{AR}{\beta E}) \tag{12}$$

For n = 1, $g(\alpha) = -\ln[(1-\alpha)/T^2]$, and from the most linear fitting region of $\ln[g(\alpha)]$ vs. 1/T, the activation energy and the frequency factor A can be determined.

2.2. Swelling

2.2.1. Swelling at saturation (Q_∞) and rubber volume fraction (V_r)

Equation 13 represent the swelling at saturation Q_∞. It is given by

$$Q_\infty = \frac{m_2 - m_1}{m_1} \times 100 \tag{13}$$

where m_1 is the non-swollen sample mass (gm), and m_2 is the swollen sample mass at saturation.

The rubber volume fraction (Eq 14) is related to the swelling at saturation using

$$V_r = \frac{1}{1 + Q_\infty \frac{\rho_r}{\rho_s}} \tag{14}$$

where ρ_r and ρ_s represents the rubber and solvent densities respectively (ρ EPDM = 0.92 gm/cm^3, ρ toulene = 0.87 gm/cm^3). From the values of rubber volume fraction one can determine the value of crosslink density ve directly using Flory-Rehner equation. In a previous study, the cross-link density of the samples was calculated [25].

2.2.2. Kraus and Cunneen-Russel models

These theoretical models predict the interaction between the filler (borax) and rubber matrix. Kraus' equation is written as

$$\frac{V_{ro}}{V_{rf}} = 1 - m\frac{Z}{1-Z} \tag{15}$$

where V_{ro} is the rubber volume fraction for the pure gum and V_{rf} is the rubber volume fraction for the rubber loaded by the filler. Z is the volume fraction of filler in the vulcanizate. The parameter m can be obtained from the slope of Eq 15.

Another model is used; which is represented as

$$\frac{V_{ro}}{V_{rf}} = ae^{-z} + b \tag{16}$$

Equation 17 represents another form of Eq 16 in terms of the swelling of filler-reinforced vulcanizes.

$$\frac{Q_f}{Q_g} = e^{-z} + b \tag{17}$$

where Q is the amount of the solvent embedded per unit weight of the rubber, f and g refer to the filled and gum samples and a and b are two constants that depend on the filler activity. The values of the parameters a and b can be determined from the linear relation of Eqs 16 and 17. A high value of a and a low value of b indicate strong polymer attachment.

3. Experimental work

3.1. Sample preparation

Carbon-black (N-220) was used as filler in the synthetic EPDM reinforcement. In the vulcanization process, zinc oxide was used as an inorganic activator and stearic acid as an organic activator. All of these ingredients were mixed at room temperature using a two-roll mill. During mixing these ingredients, paraffin oil is gradually added as a softener (see Table 1). For simplicity, samples are coded and listed in Table 2.

Table 1. The ingredients of the EPDM rubber composite samples.

Material	Role	Amount (phr)
EPDM (local market)	Rubber base	100
Carbon-black (N-220) (Degussa)	Reinforcement (filler)	50
Paraffin oil (ZMTH-Egypt)	Softener (plastizer)	50
Steric acid (Behn Mayer)	Activator	2
ZnO (Zinc Egypt)	Activator	5
Z.K (Behn Mayer)	accelerator	3
Sulfur (Polychem-Egypt)	Curing agent	3

Table 2. The sample code and description.

Sample code	Sample description	Note
EPDM_Gm	Pure EPDM (Gum)	Pure without any additives
EPDM_C	EPDM host rubber composite	EPDM with ingredient (Table 1) without borax
EPDM_C25B	EPDM host + 25 phr Borax	EPDM with ingredient (Table 1) with 25 phr borax
EPDM_C50B	EPDM host + 50 phr Borax	EPDM with ingredient (Table 1) with 50 phr borax

The obtained master-batch was weighted and divided into equal parts, and borax (25 and 50 phr) was added to the prepared product. The composites were mixed again using the two roll mills and vulcanized (cross-linked) by a compressive method at 153 ℃ and 4 MPa. The prepared composite was compressed in the form of a circular disc with a diameter of 10 cm and a thickness of 4 mm. Figure 1 shows a photographic picture of the prepared samples.

Figure 1. A photographic picture for the prepared samples.

3.2. Thermogravimetric analysis

Thermogravimetric analysis studies were carried out using a TGA-50 (Shimadzu Company, Japan) at a heating rate of 10 ℃/min under nitrogen gas atmosphere from room temperature to 600 ℃.

4. Results and discussion

4.1. Thermogravimetric analysis (TGA)

The TGA (weight-loss) curve and its 1st derivative for EPDM gum (EPDM_Gm) in nitrogen are shown in Figure 2. The TGA curve is a one-step decomposition. The curve reveals that the weight loss is relatively small (less than 3%) in the temperature range below 200 ℃ and reaches approximately 5% at about 380 ℃. This indicates the extent of thermal stability of the material in this range of temperatures. The main decomposition stage of the sample starts at about 380 ℃ and reaches complete decomposition at temperatures above 500 ℃. The fast rate of decomposition can be noted from the sharpness of the first derivative curve, as shown in Figure 2. The temperature corresponding to the maximum decomposition rate occurs at 452 ℃ (DTGA peak). The initial loss before the onset temperature, between room temperature and 380 ℃, can be attributed to the loss of volatile components in the sample, which was neglected (<5%). The decomposition temperature range for the EPDM_Gm sample (from 380 to 500 ℃) is in agreement with other references [26,27].

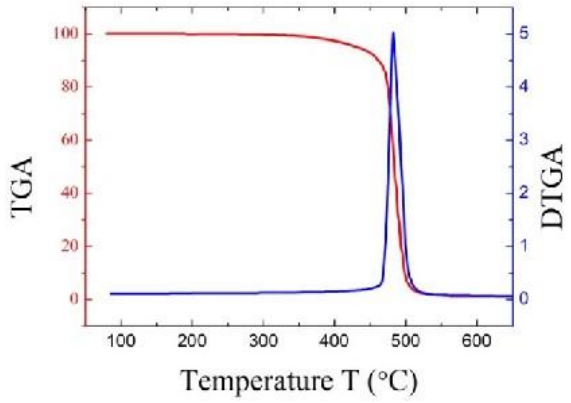

Figure 2. TGA and DTGA curves of pure EPDM gum in N_2.

Figure 3a shows a comparison between the thermal decomposition curves for EPDM_Gm and host composite sample (EPDM_C). The degradation behavior of EPDM + Gm sample is completely different from that of the host EPDM_C sample. The EPDM_C sample show less thermal stability than the EPDM_Gm sample. The T_{onset} for the EPDM_Gm sample is 437 ℃, while for the EPDM_C sample (without borax) is 264 ℃.

Figure 3b represents the DTGA curves for EPDM_Gm and EPDM_C samples. Rubber gum has only a single narrow peak, while the EPDM_C sample has more than four peaks. The main decomposition peak for gum is located at 485 ℃, while for the composite sample, it is located at 475 ℃. The additives used during the processing of the EPDM_C sample, in addition to the thermal treatment and vulcanization process, may cause a significant change in the thermal behavior of the

host polymer (EPDM_C). It is noted that the decomposition curve becomes more complex and includes several stages of decomposition besides the main decomposition stage (Figure 3b). The additive (sample ingredients) and the vulcanization process represent the main reasons for the reduction of the thermal stability of the composite host sample (EPDM_C) compared with the EPDM_Gm. The mass loss values at 400 ℃ for EPDM_Gm and EPDM_C were about 3.8% and 19%, respectively. Host rubber composite (EPDM_C) comprises volatile components such as oil, accelerators, etc. Some of these components dissolve and evaporate as volatile components through the first temperature stage (from 50 ℃ to 150 ℃). Other components are released through the second stage (from 150 ℃ to 400 ℃). It is clear that EPDM_Gm decomposes rapidly and through a narrow range of temperatures (from 410 ℃ to 480 ℃). In the case of the host sample, the EPDM decomposition peak is accompanied by a group of peaks that confirm the presence of other compounds or elements decomposed in this range of temperatures. The presence of the shoulder (or small peak) at a temperature of 418 ℃ and the broadening of the main decomposition peak of EPDM can be attributed to the fracturing of some bonds in the host rubber chains, which results in the existence of small rubber chain with free radicals. These free radicals may accelerate the decomposition of these portions, which will decompose easier than the main chains of the EPDM_Gm sample. They will appear as a superimposed peak with the principal decomposition peak. The high-temperature decomposition peaks are located beyond the main decomposition region of rubber and have a centre of maximum decomposition rates at about 525 ℃ and 550 ℃. These two peaks can be classified as strong decomposition due to non-volatile residual materials (except carbon black).

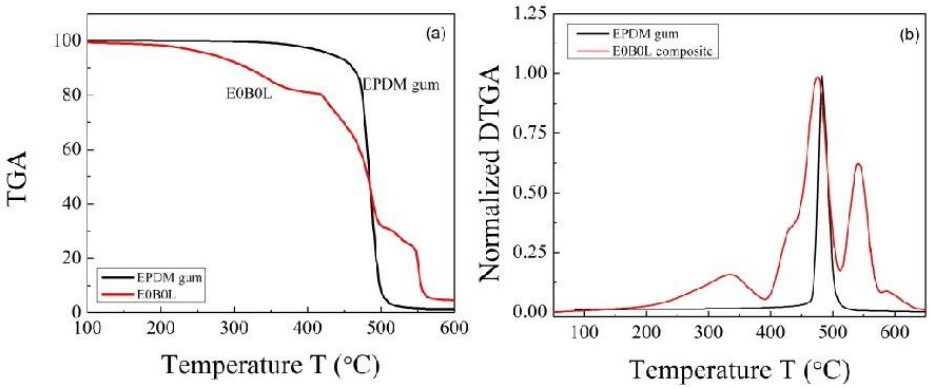

Figure 3. A comparison between (a) TGA and (b) DTGA curves of EPDM_Gm and the vulcanized EPDM_C in N_2 gas.

Figure 4 shows the TGA decomposition curves of the basic composite sample and samples loaded with different weight ratios of borax (0, 25, and 50 phr borax). The addition of borax reduces the thermal stability of the composite sample in the temperature range from 120 ℃ to 450 ℃. There are no significant changes in the decomposition phase of the host rubber (EPDM_C) (as seen in the temperature range from 450 ℃ to 500 ℃). This is an indication that the addition of borax did not affect the basic structure of the elastomer (EPDM_Gm), but it had an effective effect on the thermal decomposition of other volatile elements.

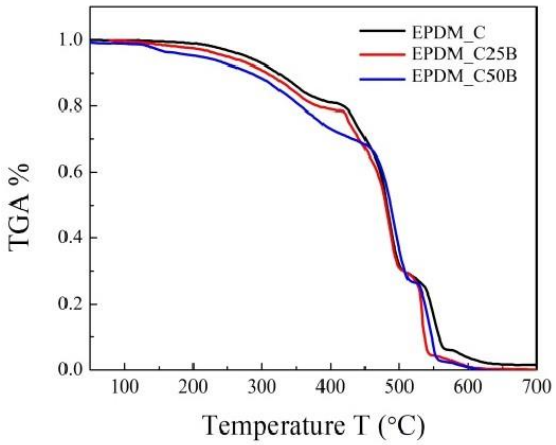

Figure 4. The TGA curves for composite sample and samples loaded with different phr of borax (0, 25, and 50 phr).

The thermal parameters extracted from the TGA data at different degradationstages are shown in Table 3. It is noticed that the $T_{5\%}$ and $T_{90\%}$ decrease with the increase in the percentage of borax.

Table 3. Some TGA thermal parameters ($T_{5\%}$, $T_{90\%}$ and T_{max}) for EPDM host composite (EPDM_C) and borax loaded composite samples (EPDMCxB).

Sample	$T_{5\%}$	$T_{90\%}$	T_{max}
EPDM_C	292.9	580.6	453.2
EPDM_C25B	242.3	549.3	430, 485
EPDM_C50B	172.3	525.2	480

Figure 5 displays the first derivative of the TGA curves for the host sample and the borax-loaded samples. It is clear from the figure that the addition of borax displacements the maximum decomposition peak at higher temperatures. The DTGA curve shape was modified for the sample loaded with 50 phr borax. The multiple peaks for the host composite and 25 phr borax were merged into three smooth peaks and separated from each other. The disappearance of the small peaks, or especially the shoulder associated with EPDM decomposition (peak 2), is evidence that the addition of borax contributed to an increase in the homogeneity of the sample and a decrease in the presence of various entanglements.

Figure 6a–c show the peak separation of the superimposed decomposition process using Origin Lab 8.0 software to get more understanding and deep information about the decomposition process. Figure 6a shows the DTGA behavior of the host composite sample (EPDM_C). The decomposition process of this composite is complex and includes many overlapping processes. There are five processes with different thermal centres (maximum decomposition rate). Some of these processes can be attributed to a well-known source. For example, the components or compounds that are easy to volatilize and decompose appear together in the first decomposition region (blue- or 1st peak from left). The centre of the maximum decomposition rate for such a compound can be considered at a temperature of about 320 ℃, which can include paraffin oil, processing oil, curing agent, etc.

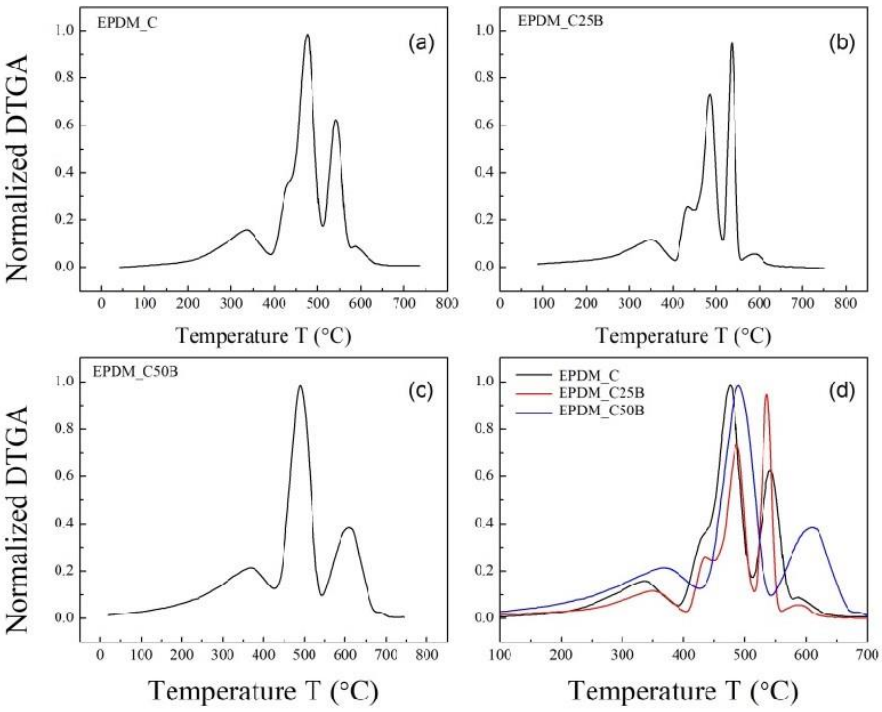

Figure 5. Normalized DTGA curves for (a) composite EPDM0B and sample loaded with (b) 25 phr borax, (c) 50 phr borax and (d) all curves of DTGA for comparison.

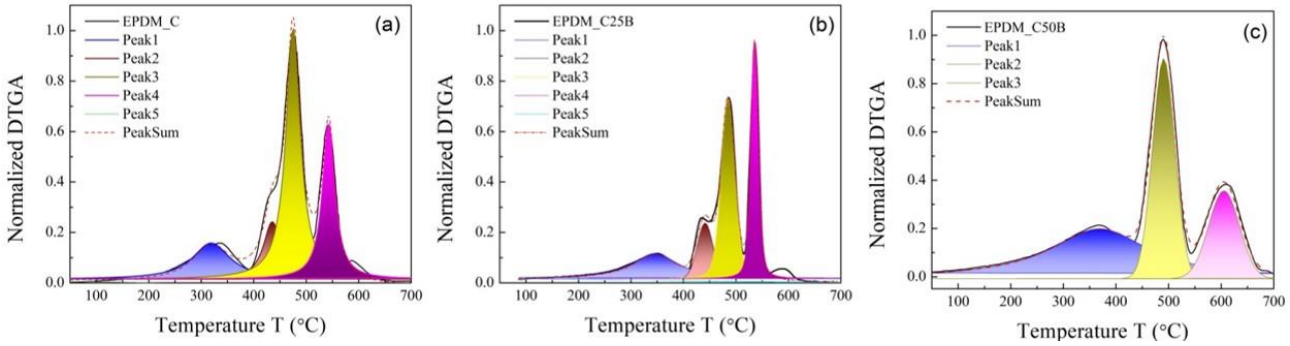

Figure 6. Peak separation for host composite and composite loaded with 25 and 50 phr borax.

The presence of two convergent peaks (red and blue, or the 2nd and 3rd peaks from the left) represents the main reaction of EPDM polymer. This complex decomposition region is composed of small and large peaks. Several EPDM chains and molecules could have been partially decomposed and reflected in the small one. The second peak can be considered as the main decomposition of EPDM rubber. It is located in a thermal range that matches many previous studies. Finally, there are two other peaks (4th and 5th peaks) located beyond the main decomposition region of rubber and have a centre of maximum decomposition rates at about 550 ℃ and 600 ℃, respectively. These two peaks can be attributed to residual non-volatile materials (strong decomposition).

Those peaks determined for the host composite will be compared to those corresponding to the sample loaded with borax. Figure 6b,c show the peak separation for the decomposition process for

samples loaded with 25 and 50 phr borax, respectively. These figures show that there are three basic decomposition processes, but the presence of heterogeneity within the composite has shown some secondary processes, such as the decomposition processes of a fraction of the EPDM chains, which appears in the form of a shoulder accompanying the main decomposition process of the host rubber. Also, the appearance of a small peak at high temperatures represents the decomposition of the remaining chains. These chains are isolated by the previous combustion products. As mentioned earlier, the addition of borax supports the distribution of the sample ingredients and resolves the entanglement of the chains. This improves the DTGA curve shape.

By studying the different models that predict the values of the activation energy Ea and the exponent factor A for thermal decomposition, useful information can be obtained to clarify the thermal stability and thermal behavior of materials at high temperatures. There are several methods for determining the kinematic parameters of solid interactions. These models are useful in investigating the thermal behavior of homogeneous and heterogeneous solids and comparing the results predicted by those models.

Three different models were applied to investigate the effect of borax on the thermal behaviour of the host rubber composite. These models are the Broido model (Eqs 7 and 8), the Horowitz and Metzger model (Eqs 10 and 11) and the Coats-Redfern model (Eq 12). Figures 7–9 illustrate the application of Broido, Horowitz and Metzger and Coats-Redfern models for the main decomposition stage (region II), respectively. According to each model, both the activation energy and the exponent factor A are calculated and listed in Table 3.

Horowitz and Metzger have higher activation energies in five of the nine comparisons than Coats-Redfern by about 15%. Comparing Broida with Coats-Redfern, four are less than 15% different. However, we observed convergence in the overwhelming majority of activation energies calculated by these models. The values of A's factors calculated from the Horowitz and Metzger and Coats-Redfern models are close to each other. The largest difference was found in the Broido model values.

There are different mathematical treatments applied to each of these three models, which can explain fluctuations in activation energy calculations. This appears in the difference in straight region extension. By reviewing the linear regions for each case, it will be noticed that there is congruence in some cases and differences in others (at the same stage of decomposition).

In an attempt to correlate the change in the activation energy of thermal decomposition with the rate of decomposition, let us consider (for example) the third decomposition stage for the three samples (the host composite and composite loaded with borax). Compared to the other samples loaded with borax, the host rubber composite sample has a lower decomposition rate (decomposition rate is the slope of the straight region of the TGA curve during decomposition). The fastest decomposition was for the sample loaded with 25 phr borax. By comparing the activation energy values in Table 4, it is observed that the sample with 25 phr borax has the largest activation energy of the three models. This is followed by 50 phr borax, followed by the host rubber composite sample. This means that the addition of 25 phr borax was the optimal amount to interact with the EPDM rubber chains. In the case of 50 phr borax, the borax residue (which did not react with the rubber chains) reduced the average decomposition activation energy.

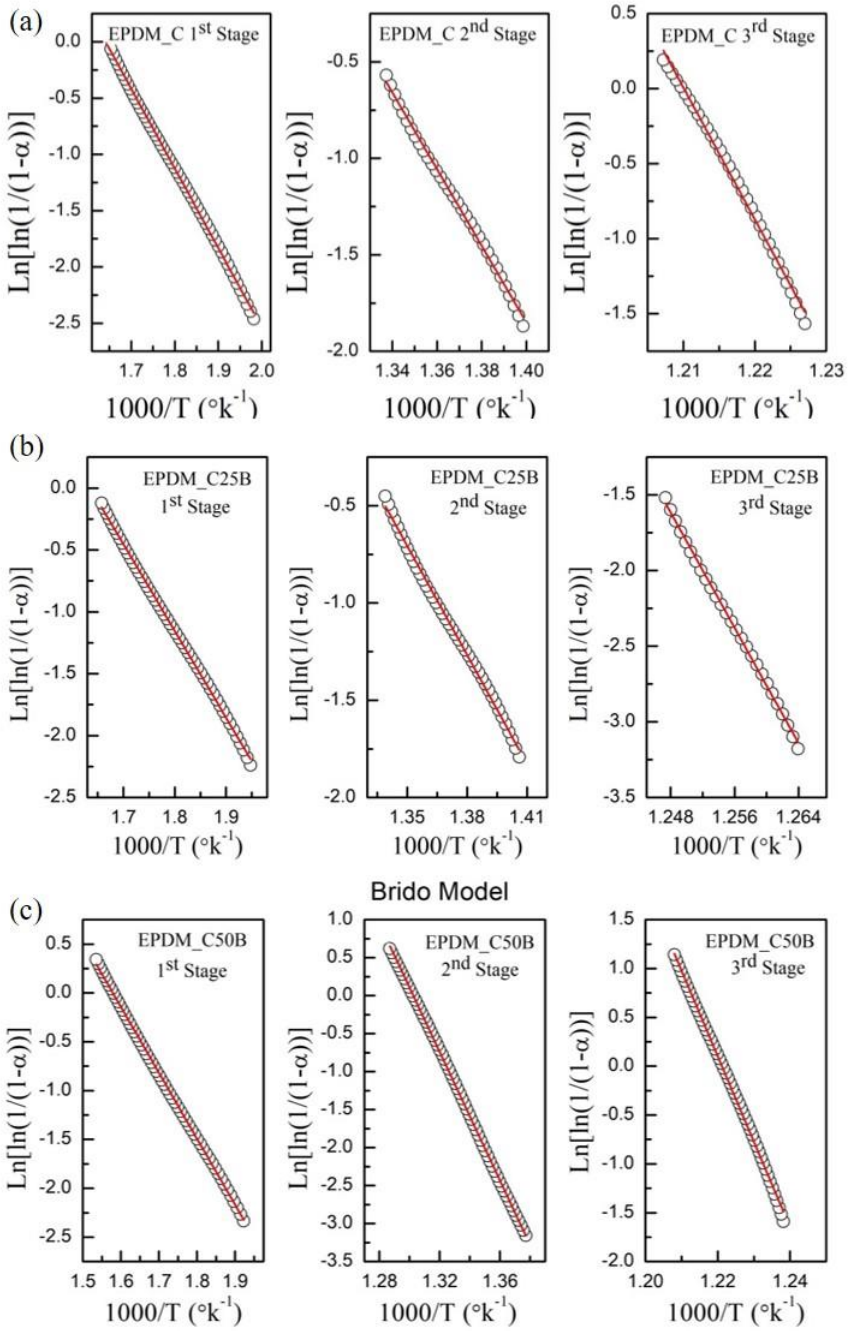

Figure 7. Linear fitting by Broido's model for (a) EPDM composite, (b) EPDM composite/25 phr borax, (c) EPDM composite/50 phr borax.

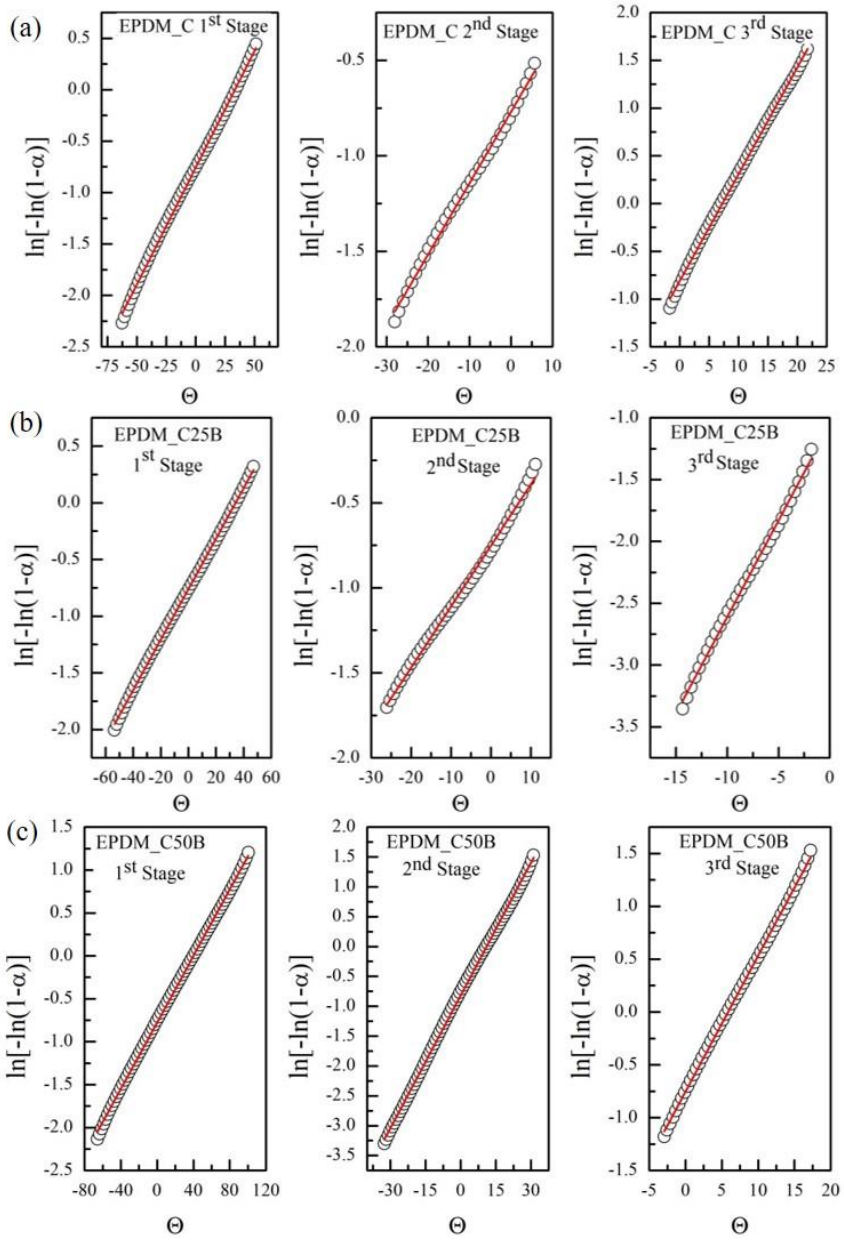

Figure 8. Linear fitting by Horowitz and Metzger model for (a) EPDM composite, (b) EPDM composite/25 phr borax, (c) EPDM composite/50 phr borax.

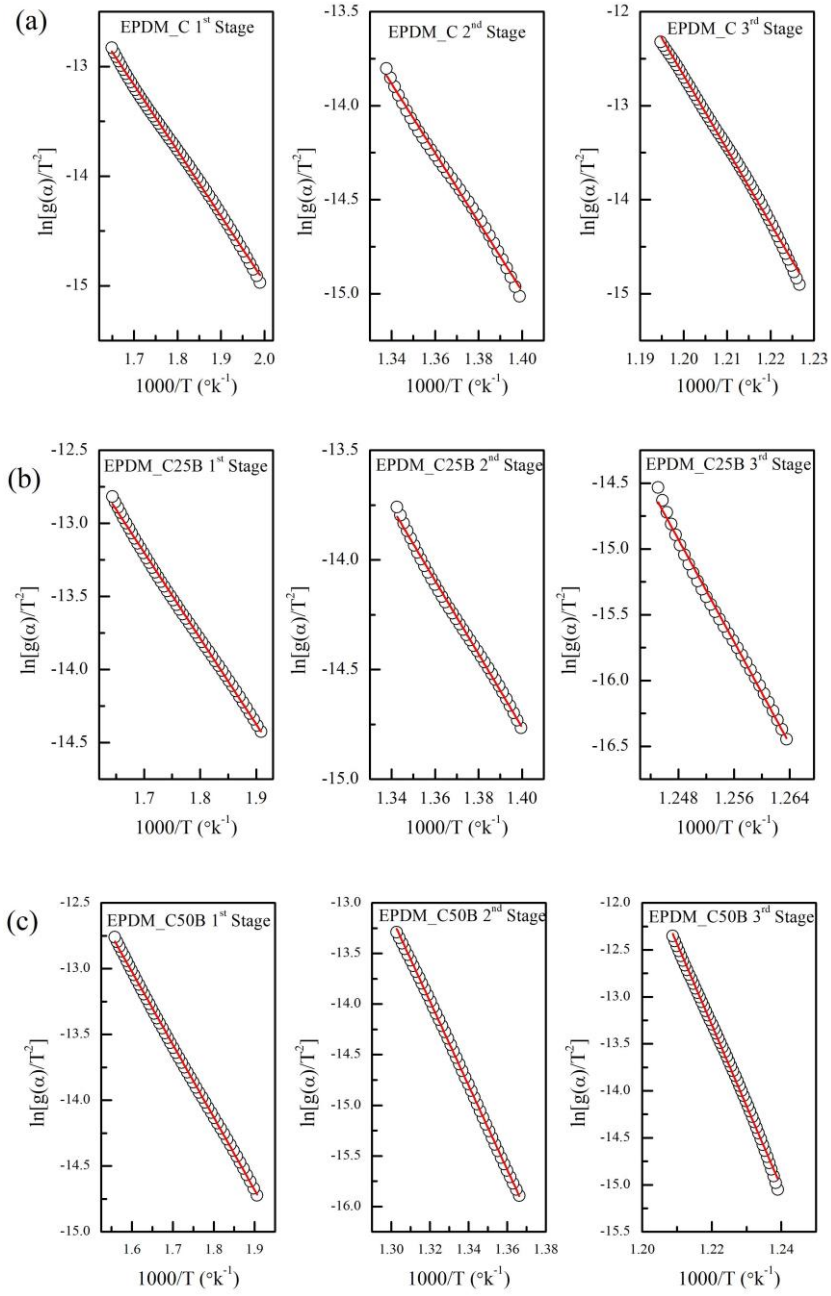

Figure 9. Linear fitting by Coats-Redfern model for (a) EPDM composite, (b) EPDM composite/25 phr Borax, (c) EPDM composite/50 phr borax.

Table 4. The calculated activation energy and predicted exponent factor for host rubber and rubber loaded with 25 and 50 phr borax.

E	Stages	Horowitz and Metzger				Broido				Coats Redfern				E (average)
		Slope	Intercept	E (kJ/mol)	A	Slope	Intercept	E (kJ/mol)	A	Slope	Intercept	E (kJ/mol)	A	
0 B	1st	7.05	11.57	57.69	3.6×10^{3}	7.08	11.63	58.86	1.3×10^{8}	6	3	49.9	2.0×10^{4}	55.5
	2nd	20.15	26.34	176.12	1.5×10^{10}	19.86	25.95	165.12	6.2×10^{14}	18.4	10.8	153	1.5×10^{8}	164.8
	3rd	81.1	98.12	611.5	3.9×10^{48}	88	106.42	727.63	2.4×10^{50}	79	82.1	656.8	6.0×10^{39}	666.5
25 B	1st	6.98	11.4	60.8	2.7×10^{3}	7	11.47	58.2	1.1×10^{8}	5.9	3.2	49.1	2.4×10^{4}	56.7
	2nd	18.23	23.9	163	4.2×10^{9}	18.7	24.54	159.47	1.4×10^{14}	16.7	8.7	138.8	1.6	154.8
	3rd	100.1	123.32	839.7	2.7×10^{53}	95.28	117.3	792.16	1.4×10^{55}	97.2	106.3	808.1	2.4×10^{5}	821.4
50 B	1st	6.73	10.6	56.3	6.3×10^{2}	6.75	10.66	56.12	4.8×10^{7}	5.5	4.1	46	5.8×10^{4}	56.2
	2nd	42.57	55.45	352.9	6.3×10^{22}	42.3	55.11	351.68	6.1×10^{27}	41.6	40.9	345.6	4.0×10^{21}	351.9
	3rd	89.6	109.4	813.11	1.2×10^{44}	87.5	106.9	731.48	3.9×10^{50}	86.4	92.1	718.1	1.4×10^{44}	758.9

The addition of borax did not significantly affect the activation energy of decomposition for the 1st stage (the volatilized components) (no interaction between such components and borax atoms). The range of activation energies for this stage was between 46 and 61 kJ/mol for the applied models. Also, through each model, the energy of decomposition for this stage was nearly independent of the addition of borax (as its average for the Horowitz and Metzger model is about 58 kJ/mol, in the Broido model about 57.8 kJ/mol and in the Coats-Redfern model about 48.4 kJ/mol).

Different equations representing the decomposition mechanisms of solid materials were used to identify the most common decomposition mechanisms applicable to our case. Our goal was to determine the closest mechanism to describe how EPDM host composites and composites loaded with borax decompose. Figure 10 summarizes a number of equations illustrating decomposition mechanism. Most of them do not give a straight line for the main decomposition region or give unacceptable values (very large) that are far from practical results and references (excluded). It was noticed from the figure that the Avrami-Erofeev equation (first-order decomposition) is the most reliable of these mechanisms that can be used to compare its results with the models studied.

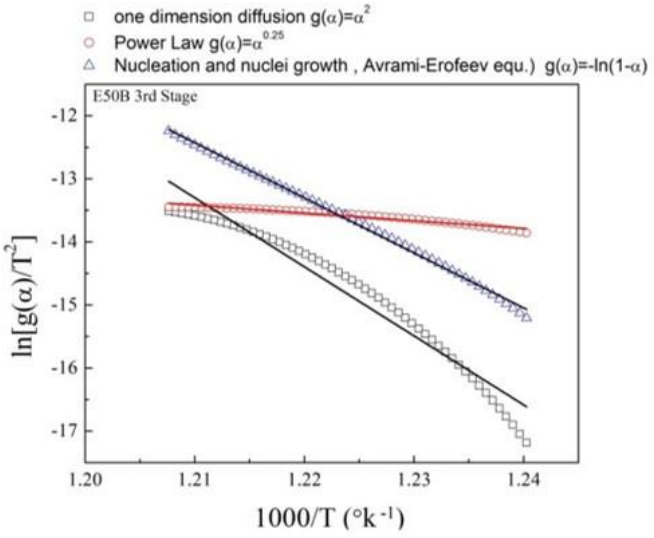

Figure 10. Application of some degradation mechanism equations.

4.2. Swelling measurement

As indicated in Table 5, drawing relations (15), (16), or (17) giving scattered points (not straight lines) fails to satisfy Kraus or Cunnen-Russel, models. We can conclude that there is no interaction between the filler (borax) and the EPDM rubber composite. This is expected because the addition of borax to the samples had no significant effect on the rubber volume fraction Vr and cross-link density [26]. This has also been observed from the measured values of mass for samples containing (0, 25, 50, 75, and 100 phr borax) i.e. no significant increase in the mass of the samples although the concentration of borax increased. This can be explained as an increase in borax and the expulsion of a similar amount of rubber.

Table 5. The calculated swelling parameters (Vr rubber volume fraction, Z filler volume fraction and swelling at saturation).

Sample	m_1 (gm)	m_2 (gm)	Vr	Q∞	Z	e − z	$\frac{Z}{1-Z}$	$\frac{V_{ro}}{V_{rf}}$	$\frac{Q_{\infty f}}{Q_{\infty g}}$
0 phr Borax	0.3	0.58	0.5	91.71	0	1	0	1	1
25 phr Borax	0.28	0.54	0.54	78.95	0.037	0.964	0.038	0.926	0.86
50 phr Borax	0.32	0.6	0.5	88.72	0.037	0.964	0.038	1	0.967
75 phr Borax	0.34	0.6	0.51	78.06	0.074	0.929	0.08	0.98	0.85
100 phr	0.33	0.59	0.52	76.49	0.055	0.946	0.058	0.96	0.834

5. Conclusions

The effect of adding borax on the thermal stability and kinetic analysis of the EPDM composite (host rubber composite) was investigated in this study. The predicted values for the activation energy (Ea) and the frequency factor (A) for the main decomposition stages of the TGA curve were determined. Three different models were applied to investigate the kinetics of thermal analysis: the Horowitz-

Metzger model, the Broido model, and the Coats-Redfern model. The activation energies predicted using these models are almost equal. The values of the frequency factor are close to each other for those derived from the Horowitz and Metzger and Coats-Redfern models. The difference was found in the Broido model values. The variations in the calculated values from these models are attributed to the different mathematical treatments followed by each. The host rubber composite sample has the lowest decomposition rate than the other samples loaded with borax (decomposition rate is the slope of the straight region of the decomposition stage of the TGA curve). While the fast decomposition rate was for the sample loaded with 25 phr borax. The sample with 25 phr borax has the largest activation energy calculated from the three models. It is followed by 50 phr borax, and then the host rubber composite sample. The activation energy of decomposition for the first stage (the volatilized parts) was not significantly affected by borax. The range of activation energies for this stage was between 46 and 61 kJ/mol for the applied models.

Use of AI tools declaration

The authors declare they have not used Artificial Intelligence (AI) tools in the creation of this article.

Conflict of interest

The authors declare that there is no conflict of interest.

References

1. Farajpour T, Bayat Y, Abdollahi M, et al. (2015) Effect of borax on the thermal and mechanical properties of ethylene-propylene-diene terpolymer rubber-based heat insulator. *J Appl Polym Sci* 132: 41936. https://doi.org/10.1002/app.41936
2. Cavdar AD, Mengeloğlu F, Karakus K (2015) Effect of boric acid and borax on mechanical, fire and thermal properties of wood flour filled high density polyethylene composites. *Measurement* 60: 6–12. https://doi.org/10.1016/j.measurement.2014.09.078
3. Kumar R, Gunjal J, Chauhan S (2022) Effect of borax-boric acid and ammonium polyphosphate on flame retardancy of natural fiber polyethylene composites. *Maderas Cienc Tecnol* 24. http://dx.doi.org/10.4067/s0718-221x2022000100434
4. Dolotina CDC, Bo-ot LMT (2022) Effect of borax and boric acid on thermal and flammability properties of rice husk reinforced recycled HDPE composite. *Athens J Technol Eng* 9: 43–60.
5. Wang J, Cao M, Li J, et al. (2022) Borate-modified, flame-retardant paper packaging materials for archive conservation. *J Renew Mater* 10: 1125–1136. http://dx.doi.org/10.32604/jrm.2022.018147
6. Orhan R, Aydoğmuş E, Topuz S, et al. (2021) Investigation of thermo-mechanical characteristics of borax reinforced polyester composites. *J Build Eng* 42: 103051. https://doi.org/10.1016/j.jobe.2021.103051
7. Abdulrahman ST, Ahmad Z, Thomas S, et al. (2020) Viscoelastic and thermal properties of natural rubber low-density polyethylene composites with boric acid and borax. *J Appl Polym Sci* 137: 49372. https://doi.org/10.1002/app.49372

8. Habeeb SA, Hasan AS, Ţălu Ş, et al. (2021) Enhancing the properties of styrene-butadiene rubber by adding borax particles of different sizes. *Iran J Chem Chem Eng* 40: 1616–1629. https://doi.org/10.30492/ijcce.2020.40535
9. Takeno H, Inoguchi H, Hsieh WC (2020) Mechanical and structural properties of cellulose nanofiber/poly(vinyl alcohol) hydrogels cross-linked by a freezing/thawing method and borax. *Cellulose* 27: 4373–4387. https://doi.org/10.1007/s10570-020-03083-z
10. More CV, Alsayed Z, Badawi MS, et al. (2021) Polymeric composite materials for radiation shielding: a review. *Environ Chem Lett* 19: 2057–2090. https://doi.org/10.1007/s10311-021-01189-9
11. Xu XR, Wu JQ, Xu J, et al. (2022) Preparation of flexible rubber composites with high contents of tungsten powders for gamma radiation shielding. *Rare Metals* 41: 2243–2248. https://doi.org/10.1007/s12598-021-01958-z
12. Sayyed MI, Al-Ghamdi H, Almuqrin AH, et al. (2022) A study on the gamma radiation protection effectiveness of nano/micro-MgO-reinforced novel silicon rubber for medical applications. *Polymers* 14: 2867. https://doi.org/10.3390/polym14142867
13. Abdulrahman ST, Patanair B, Vasukuttan VP, et al. (2022) High-density polyethylene/EPDM rubber blend composites of boron compounds for neutron shielding application. *Express Polym Lett* 16: 558–572. https://doi.org/10.3144/expresspolymlett.2022.42
14. Özdemir T, Yılmaz SN (2018) Mixed radiation shielding via 3-layered polydimethylsiloxane rubber composite containing hexagonal boron nitride, boron (III) oxide, bismuth (III) oxide for each layer. *Radiat Phys Chem* 152: 17–22. https://doi.org/10.1016/j.radphyschem.2018.07.007
15. Özdemir T, Yılmaz SN (2018) Hexagonal boron nitride and polydimethylsiloxane: a ceramic rubber composite material for neutron shielding. *Radiat Phys Chem* 152: 93–99. https://doi.org/10.1016/j.radphyschem.2018.08.008
16. Gamlin C, Markovic MG, Dutta NK, et al. (2000) Structural effects on the decomposition kinetics of EPDM elastomers by high-resolution TGA and modulated TGA. *J Therm Anal Calorim* 59: 319–336. https://doi.org/10.1023/A:1010164702571
17. Alamgir M, Ghauri FA, Khan WQ, et al. (2021) Study of thermal behaviour of EPDM/SBR blends and carbon nanocoatings deposited by sputtering. *Key Eng Mater* 875: 116–120. https://doi.org/10.4028/www.scientific.net/KEM.875.116
18. El-Nemr KF, Hassan MM, Masoaud EM, et al. (2021) Ablation and thermal properties of ethylene propylene diene rubber/carbon fiber composites cured by ionizing radiation for heat shielding applications. *Egypt J Chem* 64: 1471–1479. https://doi.org/10.21608/EJCHEM.2020.46989.2955
19. Kissinger HE (1957) Reaction kinetics in differential thermal analysis. *Anal Chem* 29: 1702–1706. https://doi.org/10.1021/ac60131a045
20. Friedman HL (1964) Kinetics of thermal degradation of char-forming plastics from thermogravimetry. Application to a phenolic plastic. *J Polym Sci Pol Sym* 6: 183–195. https://doi.org/10.1002/polc.5070060121
21. Ozawa T (1965) A new method of analyzing thermogravimetric data. *B Chem Soc Jpn* 38: 1881–1886. https://doi.org/10.1246/bcsj.38.1881
22. Ozawa T (1970) Kinetic analysis of derivative curves in thermal analysis. *J Therm Anal* 2: 301–324. https://doi.org/10.1007/BF01911411
23. Horowitz HH, Metzger G (1963) A new analysis of thermogravimetric traces. *Anal Chem* 35: 1464–1468. https://doi.org/10.1021/ac60203a013

24. Sahoo A, Kumar S, Mohanty KA (2022) A comprehensive characterization of non-edible lignocellulosic biomass to elucidate their biofuel production potential. *Biomass Convers Bior* 12: 5087–5013. https://doi.org/10.1007/s13399-020-00924-6
25. Ebrahiem A, El-Khatib AM, Doma AS (2023) Effect of lead and borax powder on the swelling behavior of EPDM rubber composite in toluene. *Egypt J Chem*. https://doi.org/10.21608/ejchem.2023.171647.7133
26. Ginic-Markovic M, Choudhury NR, Dimopoulos M, et al. (1998) Characterization of elastomer compounds by thermal analysis. *Thermochim Acta* 316: 87–95. https://doi.org/10.1016/S0040-6031(98)00290-1
27. Wu K, Wang X, Xu Y, et al. (2020) Flame retardant efficiency of modified para-aramid fiber synergizing with ammonium polyphosphate on PP/EPDM. *Polym Degrad Stabil* 172: 109065. https://doi.org/10.1016/j.polymdegradstab.2019.109065

AIMS Press